

Non-hypervascular hepatobiliary phase hypointense nodules on Gd-EOB-DTPA-enhanced MRI as a risk factor for intrahepatic distant recurrence of hepatocellular carcinoma after radiofrequency ablation

(肝細胞癌に対するラジオ波焼灼療法後の肝内他部位再発に寄与する因子としての Gd-EOB-DTPA 造影 MRI の肝細胞相における低信号結節の検討)

千葉大学大学院医学薬学府

先端医学薬学専攻

(主任：露口利夫 講師)

井上将法

Abstract

Background and aims: Gadolinium-ethoxybenzyl-diethylenetriamine pentaacetic acid (Gd-EOB-DTPA)-enhanced magnetic resonance imaging (MRI) performed before curative therapy for hepatocellular carcinoma (HCC) can distinguish between intrahepatic distant recurrence and hypervascularization. We aimed to retrospectively evaluate the presence of non-hypervascular hypointense nodules on hepatobiliary phase images (HBPI) from Gd-EOB-DTPA-enhanced MRI as a risk factor of the intrahepatic distant recurrence of early-stage HCC following radiofrequency ablation (RFA).

Methods: A total of 132 patients who underwent preprocedural Gd-EOB-DTPA-enhanced MRI followed by initial RFA were retrospectively analyzed. Post-RFA intrahepatic distant recurrence, which excluded the hypervascularization of non-hypervascular hypointense nodules detected by preprocedural Gd-EOB-DTPA-enhanced MRI, was evaluated according to the presence of non-hypervascular hypointense nodules on preprocedural Gd-EOB-DTPA-enhanced MRI.

Results: Intrahepatic distant recurrence rates following RFA were higher in patients with non-hypervascular hypointense nodules (1-year: 22.5, 2-year: 52.1%, 5-year: 89.1%) compared with in patients without non-hypervascular hypointense nodules (1-year: 7.0, 2-year: 28.8%, 5-year: 48.7%). The presence of non-hypervascular hypointense nodules was associated with markedly increased cumulative recurrence rates of both identical and different subsegment intrahepatic distant recurrence, being an independent risk factor for post-RFA identical and different subsegment intrahepatic distant recurrence (identical: HR = 2.365, $P = 0.027$. different: HR = 3.276, $P < 0.001$).

Conclusion: The presence of non-hypervascular hypointense nodules on HBPI from Gd-EOB-DTPA-enhanced MRI obtained prior to RFA is an important predictive factor of intrahepatic distant recurrence following RFA of HCC.

Keywords: hepatocellular carcinoma; Gd-EOB-DTPA-enhanced MRI; non-hypervascular hypointense nodule; radiofrequency ablation; recurrence; hypervascularization

Introduction

Hepatocellular carcinoma (HCC) is the sixth most common cancer and third leading cause of cancer-related deaths worldwide, with about 667,000 new cases per annum [1]. Although surveillance systems of high-risk populations, radiological examination, and treatment methods have been developed and improved, most HCC patients suffer from the relapse even after curative therapy, resulting in a poor prognosis [2-4].

The newly introduced magnetic resonance imaging (MRI) contrast agent, gadolinium-ethoxybenzyl-diethylenetriamine pentaacetic acid (Gd-EOB-DTPA), has enabled the concurrent assessment of tumor vascularity and unique hepatocyte specific contrast during the acquisition of hepatobiliary phase images (HBPI) [5-9]. Gadoteric acid is taken up by organic anion transporting polypeptide (OATP) B1/8 transporters into the hepatocytes [10-11]. OATP B1/8 expression gradually decreases during the process of hepatocarcinogenesis. Thus, borderline hepatocellular nodules that have potential to progress to overt HCC appear as non-hypervascular hypointense nodules on the HBPI (i.e., hypervascularization) [12, 13]. Hypervascularization is a new concept of recurrence

and proposed after the approval of Gd-EOB-DTPA-enhanced MRI.

Recent articles demonstrated the presence of non-hypervascular hypointense nodules on HBPI from Gd-EOB-DTPA-enhanced MRI observed prior to curative therapy conferred a high risk of post-curative therapy recurrence [14,15]. Moreover, these reports may indicate that the livers of patients with non-hypervascular hypointense nodules have a high potential of carcinogenesis. However, these reports did not identify the recurrence type by distinguishing between intrahepatic distant recurrence and hypervascularization. Because non-hypervascular hypointense nodules have a high probability of hypervascularization, the carcinogenetic potential of liver parenchyma cannot be estimated without classifying intrahepatic distant recurrence and hypervascularization. Furthermore, information on intrahepatic distant recurrence in patients with or without non-hypervascular hypointense nodules are required to consider treatment and follow-up strategies for patients with non-hypervascular hypointense nodules along with hypervascular HCC. It remains controversial whether the presence of non-hypervascular hypointense nodules is a risk factor of intrahepatic distant recurrence after curative therapy. The aim of this study was to retrospectively evaluate the impact of the presence

of non-hypervascular hypointense nodules on HBPI of Gd-EOB-DTPA enhanced MRI on
intrahepatic distant recurrence after radiofrequency ablation (RFA) of early-stage HCC.

Patients and Methods

Patients

The research ethics committee of our institution approved this study (No. 2,148), and the requirement for the informed consent of treatment was waived. Medical records were retrieved for patients with HCC treated at our institution.

Patients enrolled in this study were selected using the following inclusion criteria at their initial RFA: (1) the presence of histologically confirmed or clinically diagnosed HCC (fulfilling the criteria for lesions with typical imaging) [16], (2) presence of early-stage HCC (single hypervascular HCC lesion of ≤ 50 mm or ≤ 3 hypervascular HCC lesions of ≤ 30 mm, without macrovascular invasion or extrahepatic metastasis), (3) Child–Pugh A or B, and (4) Gd-EOB-DTPA-enhanced MRI performed prior to initiation of RFA.

The RFA procedure was performed percutaneously under conscious sedation. We used real-time ultrasound guidance (Power Vision 8000, Aplio XV, Aplio XG, or Aplio 500; Toshiba, Tokyo, Japan) during insertion of the electrode. A 17-gage cooled-tip

electrode (Cool-Tip; RF Ablation System, Covidien, Boulder, Colorado, CO) was inserted into the tumor through the liver tissue, and then radiofrequency energy was delivered for 6–15 min in each application. After one to two sessions of RFA, dynamic computed tomography (CT) or Gd-EOB-DTPA-enhanced MRI was performed to evaluate the efficacy of RFA. During treatment assessment, we compared imaging findings for early, portal venous, and late phases prior to ablation and portal venous and late phases following ablation. A lesion was judged to be completely ablated when the non-enhanced area appearing in the portal venous or late phase of CT or MRI postablation covered the entire lesion shown in all early, portal venous, and late phases of CT or MRI preablation with a safety margin in the surrounding liver parenchyma [17]. To reduce local recurrence after RFA, we consider a safety of at least 5 mm.

Gd-EOB-DTPA-enhanced MRI before initial RFA

Gd-EOB-DTPA-enhanced MRI was performed prior to RFA for the diagnosis and staging of HCC in all patients. MRI was performed using a 1.5-T scanner (Intera Achieva 1.5 T Nova Dual; Philips Healthcare) with a six-channel phased-array coil as the receiver

coil, a 1.5-T scanner (Signa HDxt; GE Healthcare), or a 3-T scanner (Discovery MR 750; GE Healthcare) with a twelve-channel Torso-array coil. We obtained T1-weighted dual fast field echo images (in-phase and opposed phase) before injecting the contrast medium. Dynamic fat-suppressed T1-weighted 3D turbo field-echo images were obtained before and 23 s (arterial phase), 80 s (portal venous phase), 240 s (late dynamic phase), and 20 min (hepatobiliary phase) after the administration of the contrast agent. Breath-hold multi-shot T2-weighted images and single shot spin-echo echo-planar diffusion-weighted images (DWI) were obtained in the interval of the dynamic study. Patients received 0.025 mmol/kg body weight of gadoxetic acid (EOB Primovist; Bayer Health Yakuhin Co., Ltd., Osaka, Japan) at a rate of 2 mL/s through a cubital venous catheter, which was flushed with 20 mL of saline using a power injector.

Imaging analysis

Pretreatment Gd-EOB-DTPA-enhanced MRI, including enhanced T1- and T2-weighted images, DWI, dynamic imaging including arterial, portal venous, and late dynamic phases, as well as HBPI were retrospectively reviewed by two hepatologists specialized in HCC

(To note, our hepatologists collectively have 13 years of experience with reading Gd-EOB-DTPA-enhanced MRIs). First, the reviewers evaluated the HBPI and detected hypointense nodules in the liver. For these nodules, the relative enhanced degree of the nodules on the arterial phase images was determined with regard to whether or not hyperintensity was present. Hemangiomas and hepatic cyst identified based on classical enhancement pattern or nonenhancement on dynamic phase images and hyperintensity on T2-weighted MR images, respectively, were excluded. When imaging assessment was discordant between the two reviewers, consensus was obtained through discussion.

Follow-up and assessment of recurrence

During follow-up, tumor markers, including alfa fetoprotein (AFP) and des- γ -carboxy prothrombin, were measured every 1–2 months, and dynamic CT or Gd-EOB-DTPA-enhanced MRI was performed every 4–6 months. In case of suspected recurrence, at least two radiological imaging examinations, including dynamic CT, Gd-EOB-DTPA-enhanced MRI, contrast enhanced ultrasound (US), and/or angiographic CT, were performed to confirm diagnosis.

In this study, the development of recurrence was further defined as local recurrence, intrahepatic distant recurrence, hypervascularization, or extrahepatic recurrence. Local recurrence was defined as the reappearance of enhancing tumor tissue adjacent to the ablation zone after the achievement of treatment success [18]. Intrahepatic distant recurrence was defined as the development of new hypervascular tumors, which were not classified as non-hypervascular hypointense nodules on HBPI from pretreatment Gd-EOB-DTPA-enhanced MRI and were not adjacent to the treated site. An emerging non-hypervascular hypointense nodule detected via Gd-EOB-DTPA-enhanced MRI at the follow-up assessment was not defined as intrahepatic distant recurrence until hypervascularization was confirmed. Hypervascularization of non-hypervascular hypointense nodules on HBPI of pre-RFA Gd-EOB-MRI-enhanced MRI was defined as nodules that showed hypervascularity in arterial phase images and hypovascularity in portal venous or late phase images on at least two radiological imaging examinations, including dynamic CT, Gd-EOB-DTPA-enhanced MRI, contrast-enhanced US, and/or angiographic CT [12, 13]. The appearance of extrahepatic metastasis was also assessed on follow-up imaging.

We also categorized intrahepatic distant recurrence as being subsegmentally either identical or different relative to the subsegment of the original nodules. In this study, subsegments 1–8 correspond to the Couinaud’s segments 1–8, respectively according to the General Rules for the Clinical and Pathological Study of Primary Liver Cancer, Third English Edition [19]. When a tumor was located in two or more subsegments, the subsegment involving the major part of the tumor was considered.

Statistical analysis

The cumulative incidence of each type of recurrence was estimated using the Kaplan–Meier method. Time to intrahepatic distant recurrence was defined as the period from initial RFA until the diagnosis of such recurrence. If extrahepatic metastasis was observed before intrahepatic distant recurrence, the censoring date was defined as the last date of radiological assessment not showing such evidence of recurrence. If local recurrence or hypervascularization was treated by resection or local ablation, we continued follow-up until the initial intrahepatic distant recurrence. If local recurrence or hypervascularization was treated by other therapies, such as Transarterial chemoembolization, the censoring

date was defined as the last date of radiological assessment. Time to hypervascularization was defined as the period from initial RFA until the diagnosis of hypervascularization.

Univariate and multivariate Cox proportional-hazard regression models were used to estimate the hazard ratios for risk factors in relation to each type of recurrence. A *p* value of <0.05 was considered statistically significant. All statistical analyses were performed using SPSS statistical software (version 22; SPSS-IBM, Chicago, IL, USA). In multivariate analyses, we used the stepwise regression program. All variables indicated in the tables were included in the multivariate analysis. The results are demonstrated in the Tables.

Results

Patient characteristics at baseline

Between February 2008 and December 2012, 188 patients with HCC who received RFA for initial treatment of HCC were identified for potential inclusion in this study (Supplementary Fig. 1). Of the 132 patients who were eventually included in the study, the majority of patients were male (67%), Hepatitis C virus (HCV)-RNA-positive (67%), Child–Pugh class A (83%), and the median age was 72 years (range, 52–83) (Table 1). In 56 patients (42%), non-hypervascular hypointense nodules were detected on HBPI from pretreatment Gd-EOB-DTPA-enhanced MRI.

Intrahepatic distant recurrence after RFA according to non-hypovascular hypointense nodules

Sixty-eight patients (52%) developed intrahepatic distant recurrence during the follow-up period (median follow-up, 24.6 months (range, 1.0–70.7 months). In the 56 patients with non-hypervascular hypointense nodules, the estimated 1-, 2-, 3-, and 5-year

cumulative recurrence rates were 22.5, 52.1, 69.0, and 89.1%, respectively, compared with 7.0, 28.8, 38.7, and 48.7%, respectively, in the 76 patients without non-hypervascular hypointense nodules (Fig. 1). We also analyzed data on the identical vs. different subsegmental intrahepatic distant recurrence (Fig. 2). The estimated 1-, 2-, 3-, and 5-year cumulative identical subsegmental intrahepatic distant recurrence rates were 7.4, 22.1, 33.5, and 56.6%, respectively, in patients with non-hypervascular hypointense nodules, compared with 1.5, 11.0, 12.8, and 23.1%, respectively, in patients without non-hypervascular hypointense nodules (Fig. 2A). On the other hand, the estimated 1-, 2-, 3-, and 5-year cumulative different subsegmental intrahepatic distant recurrence rates were 20.6, 48.3, 67.3, and 83.4%, respectively, in patients with non-hypervascular hypointense nodules, compared with 5.6, 19.5, 32.9, and 39.6%, respectively, in patients without non-hypervascular hypointense nodules (Fig. 2B). Multivariate analysis showed that the cumulative incidence of intrahepatic distant recurrence was significantly higher in patients with non-hypervascular hypointense nodules than in patients without non-hypervascular hypointense nodules (Table 2). Similarly, non-hypervascular hypointense nodules on HBPI from pretreatment Gd-EOB-DTPA-enhanced MRI was an independent

risk factor of both the identical and different subsegmental intrahepatic distant recurrence (Supplementary Tables 1 and 2).

Non-hypervascular hypointense nodules and hypervascularization

The agreement rate of detecting non-hypervascular hypointense nodules via pretreatment Gd-EOB-DTPA-enhanced MRI between the two reviewers was 76.5% (101 of 132 patients). The remaining 31 patients required consensus between the two reviewers. Consequently, we confirmed 56 patients with non-hypervascular hypointense nodules, and we determined a total of 127 non-hypervascular hypointense nodules with a median size of 8 mm (range: 3-17 mm). According to follow-up radiological assessment of these 56 patients, there was an 82.1% agreement rate between the two reviewers. In the follow-up period, 30 patients (46 nodules) developed the hypervascularization of non-hypervascular hypointense nodules as detected by pretreatment Gd-EOB-DTPA enhanced MRI (a typical case is shown in Figure 3). The 1-, 2-, 3-, and 5-year hypervascularization rates were 26.1, 51.9, 57.7, and 65.4%, respectively. The median time of progression to hypervascularization was 22.4 months (95% CI, 7.7–37.1 months; Supplementary Fig. 2).

Table 3 shows the multivariate analysis of risk factors for hypervascularization in 56 patients with non-hypervascular hypointense nodules on HBPI from pretreatment Gd-EOB-DTPA-enhanced MRI. The maximum size of non-hypervascular hypointense nodules (>10 mm) was an independent predictive factor of hypervascularization.

Discussion

The present study showed that non-hypervascular hypointense nodules on HBPI from pretreatment Gd-EOB-DTPA enhanced MRI represent a risk factor of HCC intrahepatic distant recurrence. Our findings confirm observations from other investigations, extending these in several important directions. As established by the significant studies of Toyoda *et al.* and Lee *et al.*, non-hypervascular hypointense nodules are at a higher risk of recurrence after curative therapy of HCC such as hepatectomy or RFA [14, 15]. Unlike previous studies, we classified post-RFA recurrence as intrahepatic distant recurrence occurring in the liver parenchyma and hypervascularization of non-hypervascular hypointense nodules on HBPI of pre-treatment Gd-EOB-DTPA-enhanced MRI. Our results indicate that livers with non-hypervascular hypointense nodules have a high potential of carcinogenesis.

Carcinogenesis and spread from the primary tumor are widely believed to represent the two major mechanisms underlying intrahepatic recurrence of HCC [20]. The diseased liver undergoes carcinogenesis (i.e., de novo recurrence) and dissemination of the

remnant tumor cells related to the primary tumor after curative therapy, leading to intrahepatic metastasis. Toyoda *et al.* indicated that the presence of non-hypervascular hypointense nodule was a risk factor for multicentric occurrence but not for intrahepatic metastasis, which was defined based on the radiological location and pathological examination of recurring nodules relative to non-hypervascular hypointense nodules [14].

The high risk of multicentric occurrence is attributed to the high potential of carcinogenesis. According to Toyoda's study, hypervascularization of non-hypervascular hypointense nodules was classified as multicentric occurrence [14]. In contrast, we focused on intrahepatic distant recurrence, leaving out hypervascularization of non-hypervascular hypointense nodules. Intrahepatic distant recurrence in our approach was defined as recurrence in the liver parenchyma that lacked non-hypervascular hypointense nodules at pre-RFA. Specifically, intrahepatic distant recurrence included multicentric occurrence, except for the hypervascularization of non-hypervascular hypointense nodules at baseline and intrahepatic metastasis. As our study lacked pathological examination data, we could not classify multicentric occurrence and intrahepatic metastasis as well as the previous report did. This is a limitation of our study.

Conversely, hepatogenous spread of cancer cells may correlate with the local portal venous system, and notably, intrahepatic metastasis mainly occurs at the subsegment identical to that of the primary tumor. Based on this idea, anatomical resection involving the systemic removal of the hepatic spread contained in the tumor tissue is considered preferable [21, 22]. Thus, the risk of developing recurrence in the identical and different subsegments was separately analyzed in this study. Non-hypervascular hypointense nodules were found to be associated with a higher rate of intrahepatic distant recurrence at not only the different subsegment but also the identical subsegment. Taken together, differences in the incidence of intrahepatic distant recurrence between patients with or without non-hypervascular hypointense nodules was most likely not due to intrahepatic metastasis but due to potential carcinogenesis. Our results document the importance that patients with non-hypervascular hypointense nodules have high incidence of not only hypervascularization but also intrahepatic distant recurrence. This information will be clinically useful during follow-up after RFA.

In this study, the incidence of non-hypervascular hypointense nodules on HBPI from Gd-EOB-DTPA-enhanced MRI (42%, 56/132) does not concur with that identified in

previous studies (Toyoda *et al.*: 23%, 18/77; Lee *et al.*: 79%, 110/139) [14, 15]. We consider that these differences might be caused by disease etiology and treatment procedures (resection/RFA) of the study patients. The etiology linked to HCC in the patients included in our study was HCV infection, whereas the etiology in the previous study by Lee *et al.* was HBV infection [15]. In general, liver function, tumor size, and tumor number are all taken into account when choosing between resection and RFA [16]. Selection bias might affect the rate of non-hypervascular hypointense nodules developing in the study population. On the other hand, the cumulative hypervascularization rate of non-hypervascular hypointense nodules in this study is similar to that found of previous studies [12, 13]. This result suggests that the method for the detection of non-hypervascular hypointense nodules in our study was appropriate.

Our study had several other limitations in addition to its inability to distinguish between multicentric occurrence and intrahepatic metastasis. First, this study was based on a retrospective analysis, and thus, there may be selection bias of patients and differences in the interval of follow-up radiological assessments. Additionally, the number of patients was small, and this study was limited to HCC patients treated by RFA.

To note, this study was not able to assess overall survival due to a small observation period. Large scale, multicenter, and prospective studies with longer observation periods to assess the dynamics of non-hypervascular hypointense nodules detected via Gd-EOB-DTPA-enhanced-MRI are warranted.

This study confirms that rigorous and careful follow-up after treatment are required to enable the identification of not only the hypervascularization of non-hypervascular hypointense nodules but also intrahepatic distant recurrence for patients presenting with non-hypervascular hypointense nodules on HBPI from pretreatment Gd-EOB-DTPA enhanced MRI. Furthermore, the finding that livers with non-hypervascular hypointense nodules have a high potential of intrahepatic distant recurrence supports the view that current post-curative therapies, including the early detection of hypervascularization of non-hypervascular hypointense nodules and intervention, are insufficient. Treatment strategies that deteriorate a potential of carcinogenesis (i.e., nucleos(t)ide analogues for HBV or interferon-free direct acting antivirals for HCV) should be considered for these patients [23-25].

In conclusion, the presence of non-hypervascular hypointense nodules on HBPI

from Gd-EOB-DTPA-enhanced MRI obtained prior to RFA is a significant predictive factor of intrahepatic distant recurrence following RFA. Observations from preprocedure Gd-EOB-DTPA-enhanced MRI are critical to developing post-RFA management strategies in patients with early-stage HCC.

References

1. Farazi PA, DePinho RA. Hepatocellular carcinoma pathogenesis: from genes to environment. *Nat Rev Cancer*. 2006;6:674-687.
2. Llovet JM, Schwartz M, Mazzaferro V. Resection and liver transplantation for hepatocellular carcinoma. *Semin Liver Dis*. 2005;25:181-200.
3. Tung-Ping Poon R, Fan ST, Wong J. Risk factors, prevention, and management of postoperative recurrence after resection of hepatocellular carcinoma. *Ann Surg*. 2000;232:10-24.
4. Shiina S, Tateishi R, Arano T, Uchino K, Enooku K, Nakagawa H, et al. Radiofrequency ablation for hepatocellular carcinoma: 10-year outcome and prognostic factors. *Am J Gastroenterol*. 2012;107:569-577.
5. Hamm B, Staks T, Mühler A, Bollow M, Taupitz M, Frenzel T, et al. Phase I clinical evaluation of Gd-EOB-DTPA as a hepatobiliary MR contrast agent: safety, pharmacokinetics, and MR imaging. *Radiology*. 1995;195:785-792.
6. Vogl TJ, Kümmel S, Hammerstingl R, Schellenbeck M, Schumacher G, Balzer T, et

- al. Liver tumors: comparison of MR imaging with Gd-EOB-DTPA and Gd-DTPA. *Radiology*. 1996;200:59-67.
7. Kim SH, Kim SH, Lee J, Kim MJ, Jeon YH, Park Y, et al. Gadoteric acid-enhanced MRI versus triple-phase MDCT for the preoperative detection of hepatocellular carcinoma. *AJR Am J Roentgenol*. 2009;192:1675-1681.
 8. Ooka Y, Kanai F, Okabe S, Ueda T, Shimofusa R, Ogasawara S, et al. Gadoteric acid-enhanced MRI compared with CT during angiography in the diagnosis of hepatocellular carcinoma. *Magn Reson Imaging*. 2013;31:748-754.
 9. Van Beers BE, Pastor CM, Hussain HK. Primovist, Eovist: what to expect? *J Hepatol*. 2012;57:421-429.
 10. Kitao A, Matsui O, Yoneda N, Kozaka K, Shinmura R, Koda W. The uptake transporter OATP8 expression decreases during multistep hepatocarcinogenesis: correlation with gadoteric acid enhanced MR imaging. *Eur Radiol*. 2011;21:2056-2066.
 11. Kobayashi S, Matsui O, Gabata T, Koda W, Minami T, Ryu Y, et al. Intranodular signal intensity analysis of hypovascular high-risk borderline lesions of HCC that

illustrate multi-step hepatocarcinogenesis within the nodule on Gd-EOB-DTPA-enhanced MRI. *Eur J Radiol.* 2012;81:3839-3845.

12. Inoue T, Hyodo T, Murakami T, Takayama Y, Nishie A, Higaki A, et al. Hypovascular hepatic nodules showing hypointense on the hepatobiliary-phase image of Gd-EOB-DTPA-enhanced MRI to develop a hypervascular hepatocellular carcinoma: a nationwide retrospective study on their natural course and risk factors. *Dig Dis.* 2013;31:472-479.
13. Hyodo T, Murakami T, Imai Y, Okada M, Hori M, Kagawa Y, et al. Hypovascular nodules in patients with chronic liver disease: risk factors for development of hypervascular hepatocellular carcinoma. *Radiology.* 2013;266:480-490.
14. Toyoda H, Kumada T, Tada T, Ninomi T, Ito T, Sono Y, et al. Non-hypervascular hypointense nodules detected by Gd-EOB-DTPA-enhanced MRI are a risk factor for recurrence of HCC after hepatectomy. *J Hepatol.* 2013;58:1174-1180.
15. Lee DH, Lee JM, Lee JY, Kim SH, Kim JH, Yoon JH, et al. Non-hypervascular hepatobiliary phase hypointense nodules on gadoxetic acid-enhanced MRI: Risk of HCC recurrence after radiofrequency ablation. *J Hepatol.* 2015;62:1122-1130.

16. Kudo M, Izumi N, Kokudo N, Matsui O, Sakamoto M, Nakashima O, et al.
Management of hepatocellular carcinoma in Japan: Consensus-Based Clinical Practice Guidelines proposed by the Japan Society of Hepatology (JSH) 2010 updated version. *Dig Dis.* 2011;29:339-364.
17. Motoyama T, Ogasawara S, Chiba T, Higashide T, Yokota H, Kanogawa N, et al.
Coronal reformatted CT images contribute to the precise evaluation of the radiofrequency ablative margin for hepatocellular carcinoma. *Abdom Imaging.* 2014;39:262-268.
18. Goldberg SN, Grassi CJ, Cardella JF, Charboneau JW, Dodd GD 3rd, Dupuy DE, et al.
Image-guided tumor ablation: standardization of terminology and reporting criteria. *Radiology.* 2005;235:728-739
19. Liver Cancer Study Group of Japan. General Rules for the Clinical and Pathological Study for Primary Liver Cancer, Third English Edition. Tokyo; Kanehara 2010.
20. Sherman M. Recurrence of hepatocellular carcinoma. *N Engl J Med.* 2008;359:2045-2047
21. Makuuchi M, Hasegawa H, Yamazaki S. Ultrasonically guided subsegmentectomy.

Surg Gynecol Obstet. 1985;161:346-350.

22. Hasegawa K, Kokudo N, Imamura H, Matsuyama Y, Aoki T, Minagawa M, et al.
Prognostic impact of anatomic resection for hepatocellular carcinoma. *Ann Surg.* 2005;242:252-259.
23. Papatheodoridis GV, Chan HL, Hansen BE, Janssen HL, Lampertico P. Risk of hepatocellular carcinoma in chronic hepatitis B: assessment and modification with current antiviral therapy. *J Hepatol.* 2015;62:956-967.
24. Shiratori Y, Kato N, Yokosuka O, Imazeki F, Hashimoto E, Hayashi N, et al.
Predictors of the efficacy of interferon therapy in chronic hepatitis C virus infection. Tokyo-Chiba Hepatitis Research Group. *Gastroenterology.* 1997;113:558-566.
25. Kanogawa N, Ogasawara S, Chiba T, Saito T, Motoyama T, Suzuki E, et al.
Sustained virologic response achieved after curative treatment of hepatitis C virus-related hepatocellular carcinoma as an independent prognostic factor. *J Gastroenterol Hepatol.* 2015;30:1197-1204.

Table 1. Demographics and characteristics of study patients

| Demographics/characteristics | Value |
|--|--------------|
| Gender [n(%)] | |
| Male | 89 (67) |
| Female | 43 (33) |
| Age, years [n(%)] | |
| ≤72 | 69 (52) |
| >72 | 63 (48) |
| Median (range) | 72 (52-83) |
| HBV-DNA positive [n(%)] | |
| Absent | 117 (89) |
| Present | 15 (11) |
| HCV-RNA positive [n(%)] | |
| Absent | 44 (33) |
| Present | 88 (67) |
| Alcohol abuse [n(%)] | |
| Absent | 120 (91) |
| Present | 12 (9) |
| Cirrhosis [n(%)] | |
| Absent | 28 (21) |
| Present | 104 (79) |
| Child–Pugh class [n(%)] | |
| A | 109 (83) |
| B | 23 (17) |
| AST [n(%)] | |
| ≤3.0×UNL | 114 (86) |
| >3.0×UNL | 18 (14) |
| AFP [n(%)] | |
| ≤100 | 112 (85) |
| >100 | 20 (15) |
| Tumor size of hypervascular HCC, mm | |
| Maximum diameter, > 20 [n(%)] | |
| Absent | 85 (64) |
| Present | 47 (36) |
| Median (range) | 19 (6-40) |
| Tumor number of hypervascular HCC, multiple [n(%)] | |
| Absent | 95 (72) |
| Present | 37 (28) |
| Non-hypervascular hypointense nodule on HBPI [n(%)] | |
| Absent | 76(58) |
| Present | 56(42) |

Abbreviations: HBV, hepatitis B virus; HCV, hepatitis C virus; AST, aspartate aminotransferase; AFP, alpha-fetoprotein; HCC, hepatocellular carcinoma; HBPI, hepatobiliary phase image

Table 2. Uni- and multivariate analyses of intrahepatic distant recurrence following radiofrequency ablation

| Variables | Univariate analysis | | | P | Multivariate analysis | | P |
|---|---------------------|--------------|-------------|--------|-----------------------|-------------|--------|
| | n(%) | Hazard ratio | 95% C.I. | | Hazard ratio | 95% C.I. | |
| Gender, male | | | | | | | |
| Absent | 89 (67) | Reference | | | | | |
| Present | 43 (33) | 0.975 | 0.592-1.606 | 0.921 | | | |
| Age >72 years | | | | | | | |
| Absent | 69 (52) | Reference | | | | | |
| Present | 63 (48) | 1.168 | 0.725-1.883 | 0.523 | | | |
| HBV-DNA positive | | | | | | | |
| Absent | 117 (89) | Reference | | | | | |
| Present | 15 (11) | 0.753 | 0.325-1.744 | 0.508 | | | |
| HCV-RNA positive | | | | | | | |
| Absent | 44 (33) | Reference | | | | | |
| Present | 88 (67) | 1.382 | 0.825-2.315 | 0.220 | | | |
| Alcohol abuse | | | | | | | |
| Absent | 120 (91) | Reference | | | | | |
| Present | 12 (9) | 1.065 | 0.509-2.232 | 0.867 | | | |
| Child-Pugh class B | | | | | | | |
| Absent | 109 (83) | Reference | | | Reference | | |
| Present | 23 (17) | 2.104 | 1.164-3.804 | 0.014 | 2.304 | 1.272-4.174 | 0.006 |
| AST, >3 × UNL | | | | | | | |
| Absent | 114 (86) | Reference | | | | | |
| Present | 18 (14) | 1.348 | 0.686-2.649 | 0.386 | | | |
| AFP, >100 ng/mL | | | | | | | |
| Absent | 112 (85) | Reference | | | | | |
| Present | 20 (15) | 1.733 | 0.927-3.241 | 0.085 | | | |
| Maximum tumor size, >20mm | | | | | | | |
| Absent | 85 (64) | Reference | | | | | |
| Present | 47 (36) | 0.800 | 0.481-1.330 | 0.389 | | | |
| Tumor number, multiple | | | | | | | |
| Absent | 95 (72) | Reference | | | | | |
| Present | 37 (28) | 2.016 | 1.203-3.379 | 0.008 | | | |
| Non-hypervascular hypointense nodule | | | | | | | |
| Absent | 76(58) | Reference | | | Reference | | |
| Present | 56(42) | 2.763 | 1.696-4.502 | <0.001 | 2.87 | 1.759-4.681 | <0.001 |

Abbreviations: HBV, hepatitis B virus; HCV, hepatitis C virus; AST, aspartate aminotransferase; AFP, alpha-fetoprotein

Table 3. Uni- and multivariate analyses of the hypervascularization of non-hypervascular hypointense nodules

| Variables | Univariate analysis | | | p | Multivariate analysis | | |
|---|---------------------|--------------|-------------|-------|-----------------------|-------------|-------|
| | n(%) | Hazard ratio | 95% C.I. | | Hazard ratio | 95% C.I. | p |
| Gender, male | | | | | | | |
| Male | 36 (72) | Reference | | | | | |
| Female | 20 (28) | 0,889 | 0.427-1.847 | 0.752 | | | |
| Age >72 years | | | | | | | |
| Absent | 30 (54) | Reference | | | | | |
| Present | 26 (46) | 0.462 | 0.356-1.599 | 0.523 | | | |
| HBV-DNA positive | | | | | | | |
| Absent | 47 (84) | Reference | | | | | |
| Present | 9 (16) | 0.879 | 0.335-2.304 | 0.793 | | | |
| HCV-RNA positive | | | | | | | |
| Absent | 20 (28) | Reference | | | | | |
| Present | 36 (72) | 0.933 | 0.433-1.965 | 0.855 | | | |
| Alcohol abuse | | | | | | | |
| Absent | 54 (96) | Reference | | | | | |
| Present | 2 (4) | 1.740 | 0.408-7.425 | 0.454 | | | |
| Child-Pugh class B | | | | | | | |
| Absent | 48 (86) | Reference | | | | | |
| Present | 8 (14) | 0.979 | 0.341-2.813 | 0.969 | | | |
| AST, >3 × UNL | | | | | | | |
| Absent | 46 (82) | Reference | | | | | |
| Present | 10 (18) | 1.122 | 0.457-2.751 | 0.802 | | | |
| AFP, >100 ng/ml | | | | | | | |
| Absent | 45 (80) | Reference | | | | | |
| Present | 11 (20) | 2.420 | 1.095-5.347 | 0.029 | | | |
| Maximum tumor size of hypervascular HCC, >20mm | | | | | | | |
| Absent | 37 (66) | Reference | | | | | |
| Present | 19 (34) | 0.840 | 0.382-1.844 | 0.663 | | | |
| Tumor number of hypervascular HCC, multiple | | | | | | | |
| Absent | 39 (70) | Reference | | | | | |
| Present | 17 (30) | 1.772 | 0.839-3.741 | 0.134 | | | |
| Maximum tumor size of hypointense nodule, >10mm | | | | | | | |
| Absent | 34 (61) | Reference | | | Reference | | |
| Present | 22 (39) | 2.942 | 1.419-6.101 | 0.004 | 2.942 | 1.419-6.101 | 0.004 |
| Tumor number of hypointense nodule | | | | | | | |
| Absent | 26 (46) | Reference | | | | | |
| Present | 30 (54) | 1.214 | 0.589-2.504 | 0.600 | | | |

Abbreviations: HBV, hepatitis B virus; HCV, hepatitis C virus; AST, aspartate aminotransferase; AFP, alpha-fetoprotein; HCC, hepatocellular carcinoma

Fig. 1 Inoue et al.

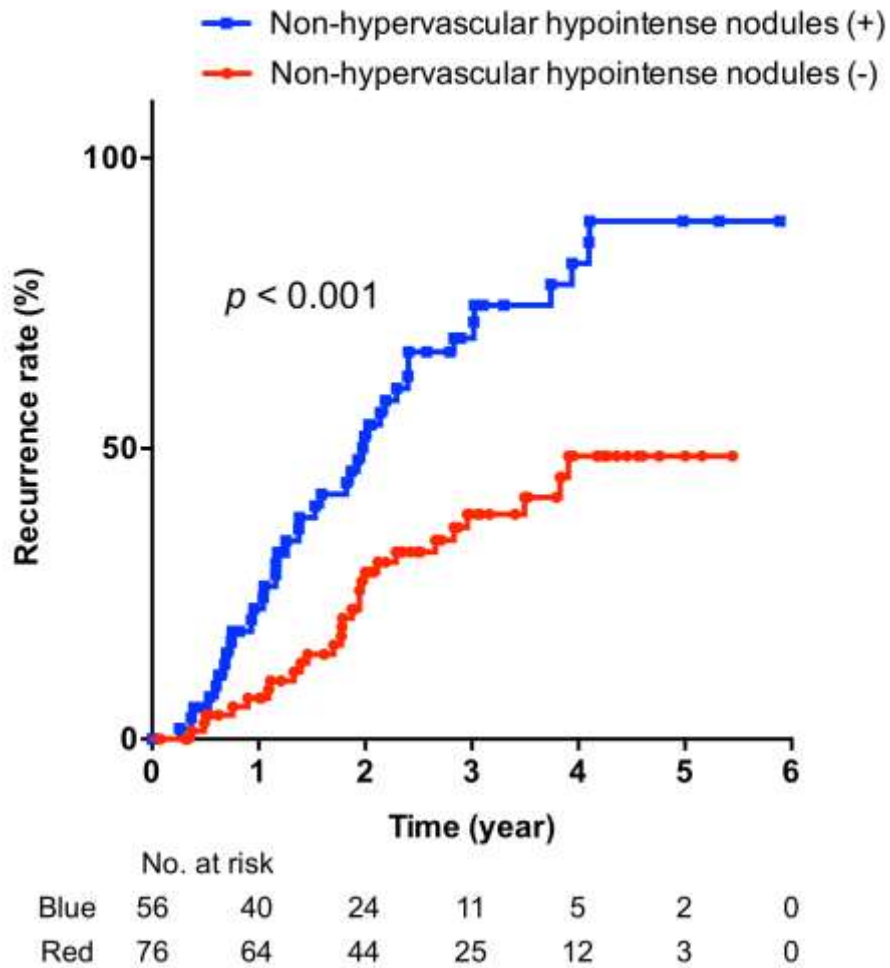


Figure 1. Kaplan–Meier curve of cumulative intrahepatic distant recurrence (blue line: presence of non-hypervascular hypointense nodules, red line: absence of non-hypervascular hypointense nodules).

Fig. 2 Inoue et al.

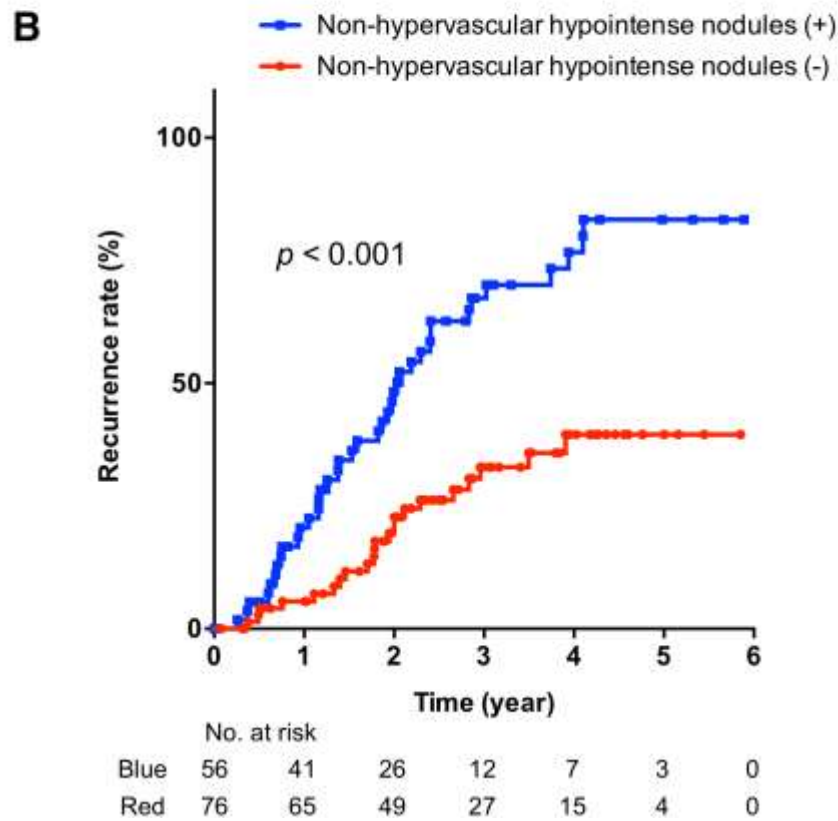
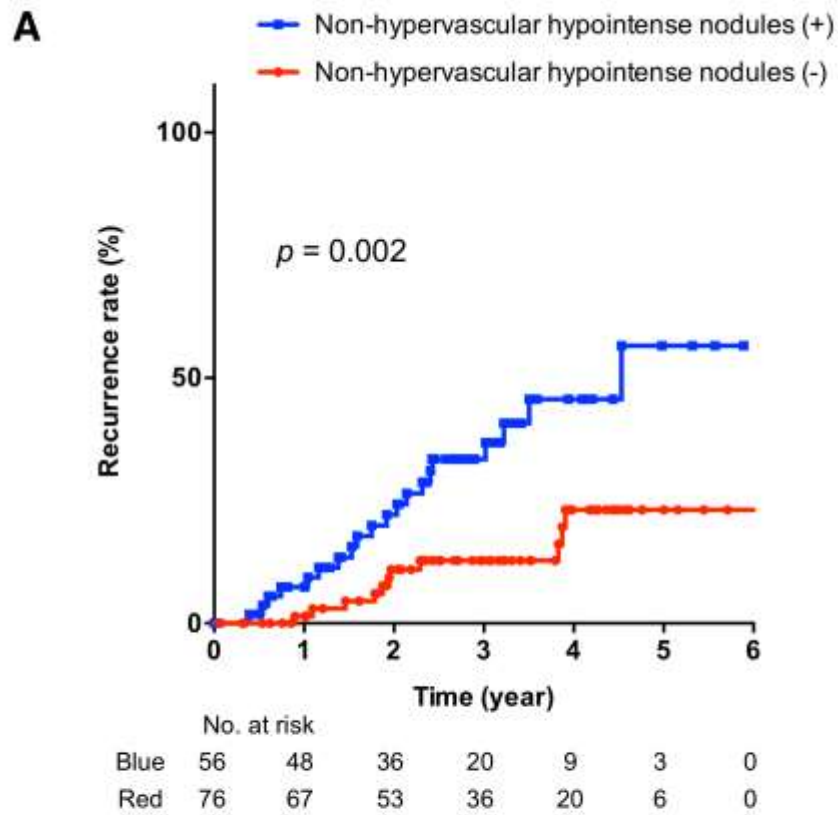


Figure 2. Kaplan–Meier curve of cumulative intrahepatic distant recurrence (blue line: presence of non-hypervascular hypointense nodules, red line: absence of non-hypervascular hypointense nodules) . A: Rates of intrahepatic distant recurrence at the identical subsegment in patients with or without concurrent non-hypervascular hypointense nodules detected during the HBPI of pre-RFA Gd-EOB-DTPA-enhanced MRI. B: Rates of intrahepatic distant recurrence at different subsegments in patients with or without concurrent non-hypervascular hypointense nodules detected during the HBPI of pre-RFA Gd-EOB-DTPA-enhanced MRI.

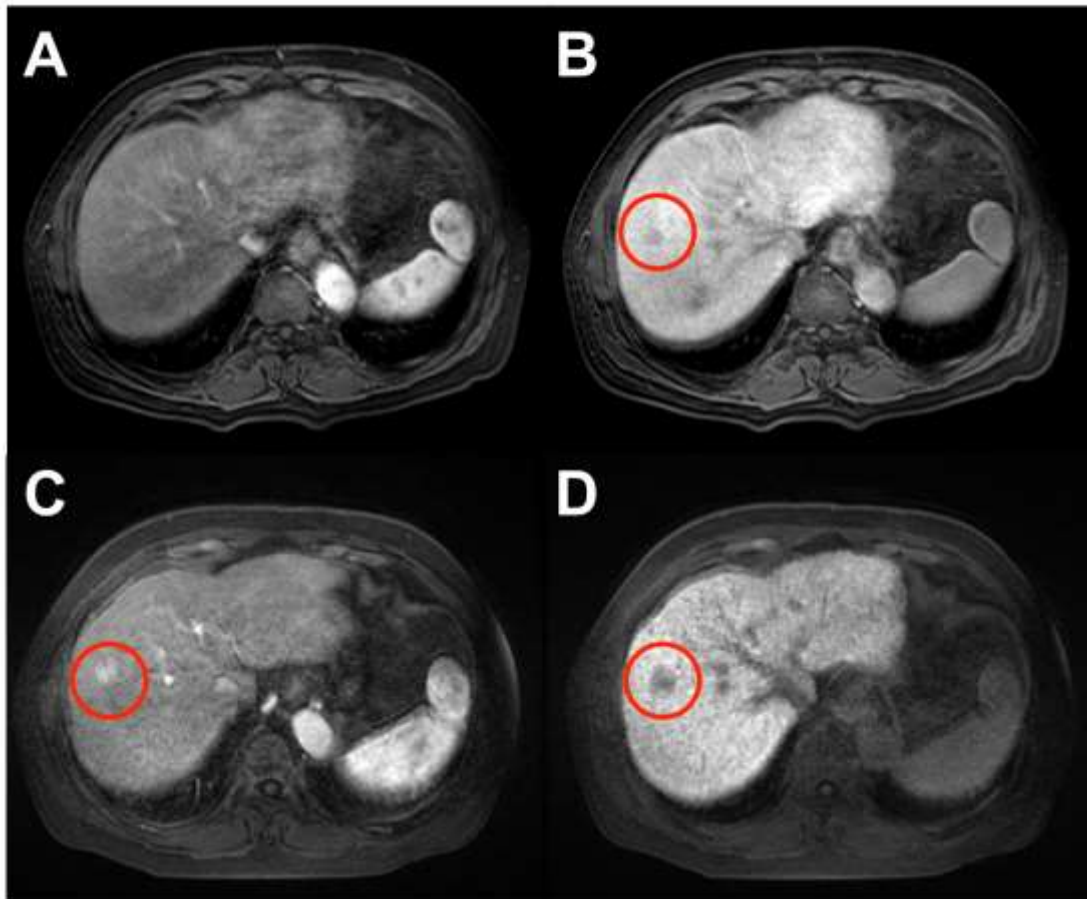


Figure 3. A representative case of hypervascularization of non-hypervascular hypointense nodules in patients with hepatocellular carcinoma as detected by gadolinium-ethoxybenzyl-diethylenetriamine pentaacetic acid (Gd-EOB-DTPA) enhanced MRI. A 61-year-old male received radiofrequency ablation (RFA) as an initial treatment for hepatocellular carcinoma (A: arterial image and B: hepatobiliary phase image (HBPI) of preprocedural Gd-EOB-DTPA-enhanced MRI). Non-hypervascular hypointense nodules were observed in another site of the liver parenchyma from which we performed RFA. Twenty-one months after RFA (C: arterial image and D: HBPI of preprocedural Gd-EOB-DTPA-enhanced MRI), hypervascularization was detected in the arterial image.

Supplementary Table 1. Uni- and multivariate analyses of identical subsegmental intrahepatic distant recurrence following radiofrequency ablation

| Variables | Univariate analysis | | | P | Multivariate analysis | | |
|---|---------------------|--------------|--------------|--------|-----------------------|--------------|--------|
| | n(%) | Hazard ratio | 95% C.I. | | Hazard ratio | 95% C.I. | P |
| Gender, male | | | | | | | |
| Absent | 89 (67) | Reference | | | | | |
| Present | 43 (33) | 0.956 | 0.457-2.002 | 0.906 | | | |
| Age >72 years | | | | | | | |
| Absent | 69 (52) | Reference | | | | | |
| Present | 63 (48) | 1.012 | 0.497-2.060 | 0.975 | | | |
| HBV-DNA positive | | | | | | | |
| Absent | 117 (89) | Reference | | | | | |
| Present | 15 (11) | 1.417 | 0.542-3.705 | 0.477 | | | |
| HCV-RNA positive | | | | | | | |
| Absent | 44 (33) | Reference | | | | | |
| Present | 88 (67) | 0.888 | 0.431-1.832 | 0.749 | | | |
| Alcohol abuse | | | | | | | |
| Absent | 120 (91) | Reference | | | | | |
| Present | 12 (9) | 0.882 | 0.268-2.907 | 0.837 | | | |
| Child-Pugh class B | | | | | | | |
| Absent | 109 (83) | Reference | | | Reference | | |
| Present | 23 (17) | 3.190 | 1.464-6.954 | 0.004 | 3.474 | 1.570-7.688 | 0.002 |
| AST, >3 × UNL | | | | | | | |
| Absent | 114 (86) | Reference | | | | | |
| Present | 18 (14) | 0.759 | 0.230-2.509 | 0.651 | | | |
| AFP, >100 ng/mL | | | | | | | |
| Absent | 112 (85) | Reference | | | Reference | | |
| Present | 20 (15) | 4.686 | 2.186-10.046 | <0.001 | 5.609 | 2.473-12.722 | <0.001 |
| Maximum tumor size, >20mm | | | | | | | |
| Absent | 85 (64) | Reference | | | Reference | | |
| Present | 47 (36) | 0.525 | 0.226-1.219 | 0.134 | 0.420 | 0.174-1.010 | 0.053 |
| Tumor number, multiple | | | | | | | |
| Absent | 95 (72) | Reference | | | | | |
| Present | 37 (28) | 2.321 | 1.122-4.801 | 0.023 | | | |
| Non-hypervascular hypointense nodule | | | | | | | |
| Absent | 76(58) | Reference | | | Reference | | |
| Present | 56(42) | 2.980 | 1.423-6.239 | 0.004 | 2.365 | 1.100-5.082 | 0.027 |

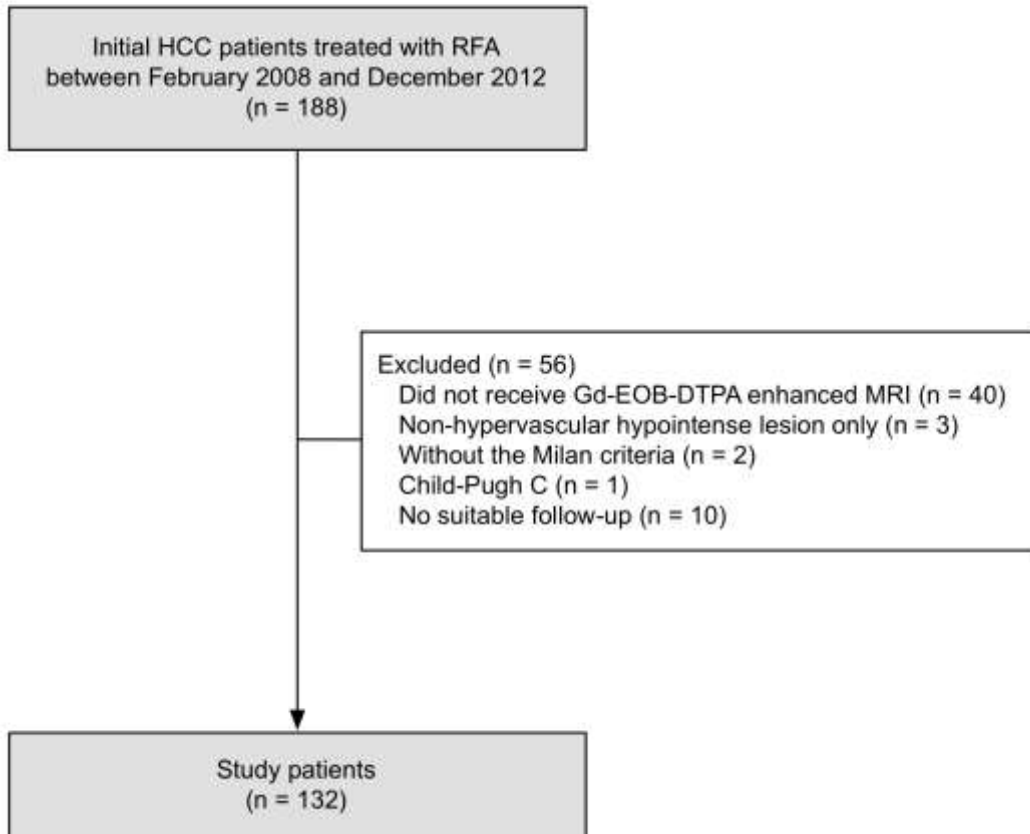
Abbreviations: HBV, hepatitis B virus; HCV, hepatitis C virus; AST, aspartate aminotransferase; AFP, alpha-fetoprotein

Supplementary Table 2. Uni- and multivariate analyses of different subsegmental intrahepatic distant recurrence following radiofrequency ablation

| Variables | Univariate analysis | | | P | Multivariate analysis | | |
|---|---------------------|--------------|-------------|--------|-----------------------|-------------|--------|
| | n(%) | Hazard ratio | 95% C.I. | | Hazard ratio | 95% C.I. | P |
| Gender, male | | | | | | | |
| Absent | 89 (67) | Reference | | | | | |
| Present | 43 (33) | 1.091 | 0.637-1.867 | 0.752 | | | |
| Age >72 years | | | | | | | |
| Absent | 69 (52) | Reference | | | | | |
| Present | 63 (48) | 1.124 | 0.679-1.860 | 0.649 | | | |
| HBV-DNA positive | | | | | | | |
| Absent | 117 (89) | Reference | | | | | |
| Present | 15 (11) | 0.612 | 0.245-1.531 | 0.294 | | | |
| HCV-RNA positive | | | | | | | |
| Absent | 44 (33) | Reference | | | Reference | | |
| Present | 88 (67) | 1.668 | 0.952-2.924 | 0.074 | 1.907 | 1.081-3.364 | 0.026 |
| Alcohol abuse | | | | | | | |
| Absent | 120 (91) | Reference | | | | | |
| Present | 12 (9) | 1.029 | 0.468-2.265 | 0.943 | | | |
| Child-Pugh class B | | | | | | | |
| Absent | 109 (83) | Reference | | | Reference | | |
| Present | 23 (17) | 1.785 | 0.947-3.365 | 0.073 | 2.189 | 1.150-4.163 | 0.017 |
| AST, >3 × UNL | | | | | | | |
| Absent | 114 (86) | Reference | | | | | |
| Present | 18 (14) | 1.626 | 0.821-3.220 | 0.163 | | | |
| AFP, >100 ng/mL | | | | | | | |
| Absent | 112 (85) | Reference | | | | | |
| Present | 20 (15) | 1.107 | 0.545-2.249 | 0.778 | | | |
| Maximum tumor size, >20mm | | | | | | | |
| Absent | 85 (64) | Reference | | | | | |
| Present | 47 (36) | 0.797 | 0.463-1.370 | 0.411 | | | |
| Tumor number, multiple | | | | | | | |
| Absent | 95 (72) | Reference | | | | | |
| Present | 37 (28) | 1.329 | 0.758-2.331 | 0.321 | | | |
| Non-hypervascular hypointense nodule | | | | | | | |
| Absent | 76(58) | Reference | | | Reference | | |
| Present | 56(42) | 3.108 | 1.840-5.248 | <0.001 | 3.276 | 1.937-5.540 | <0.001 |

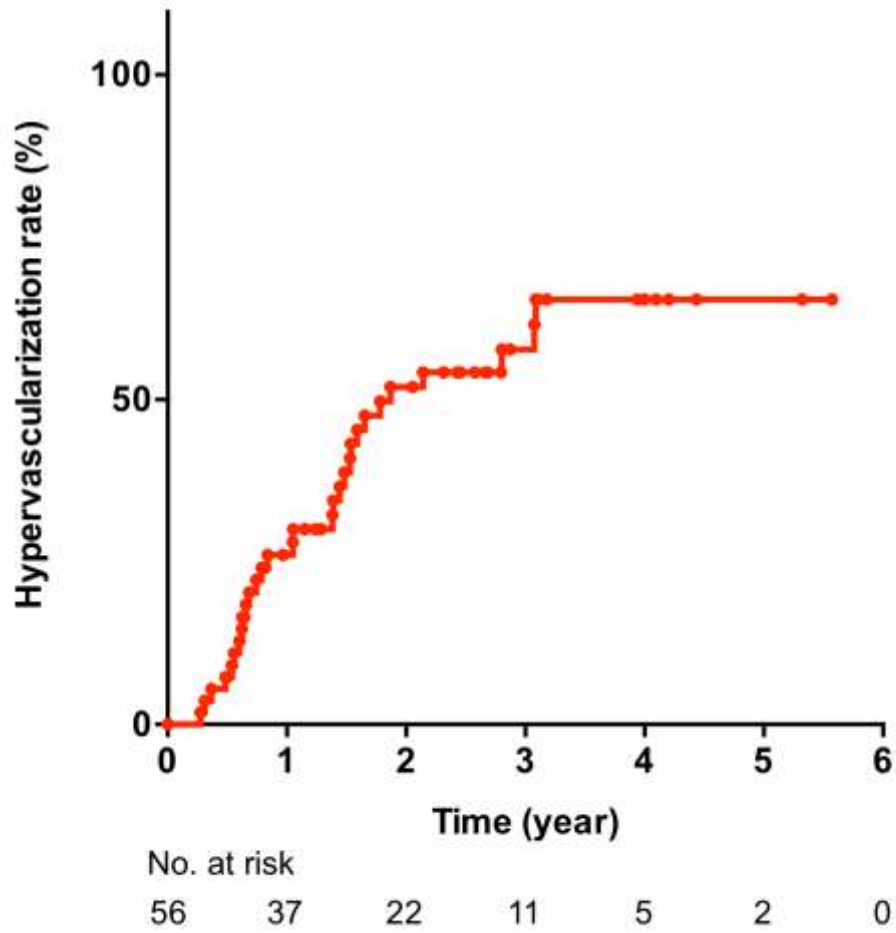
Abbreviations: HBV, hepatitis B virus; HCV, hepatitis C virus; AST, aspartate aminotransferase; AFP, alpha-fetoprotein

Supplementary Fig. 1 Inoue et al



Supplementary Figure 1. Study flow.

Supplementary Fig. 2 Inoue et al.



Supplementary Figure 2. Kaplan–Meier curve of the cumulative hypervascularization rate of non-hypervascular hypointense nodules on pre-RFA HBPI of Gd-EOB-DTPA-enhanced MRI.

Journal of Gastroenterology and Hepatology

平成28年10月18日 印刷中 (受理済み)

